Smart Materials and Devices
https://doi.org/10.70401/smd.2026.0040

Supplementary information

Iron doping P2-$Na_{2/3}Li_{1/6}Fe_{1/6}Mn_{2/3}O_2$ cathode with enhanced anionic eedox and structural stability for sodium-ion batteries

Siyu Wang, Qingmei Su, Liming Wang, Lishan Lai, Wenxin Shi, Weihao Shi, Gaohui Du

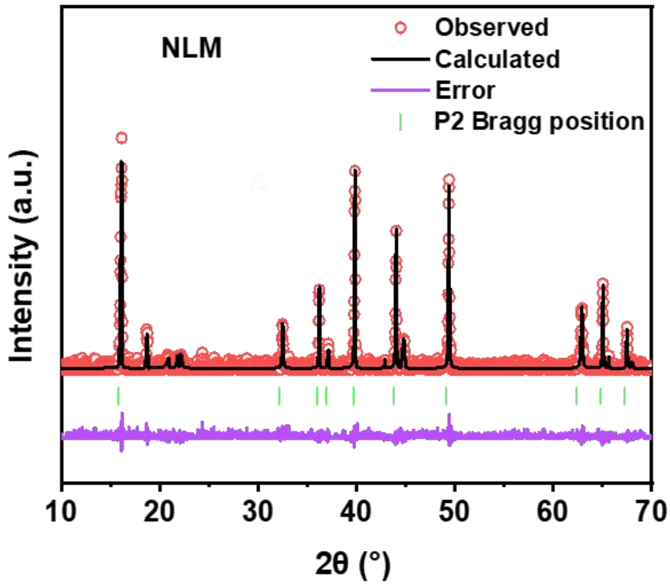

Figure S1. XRD Rietveld refinement of NLM.

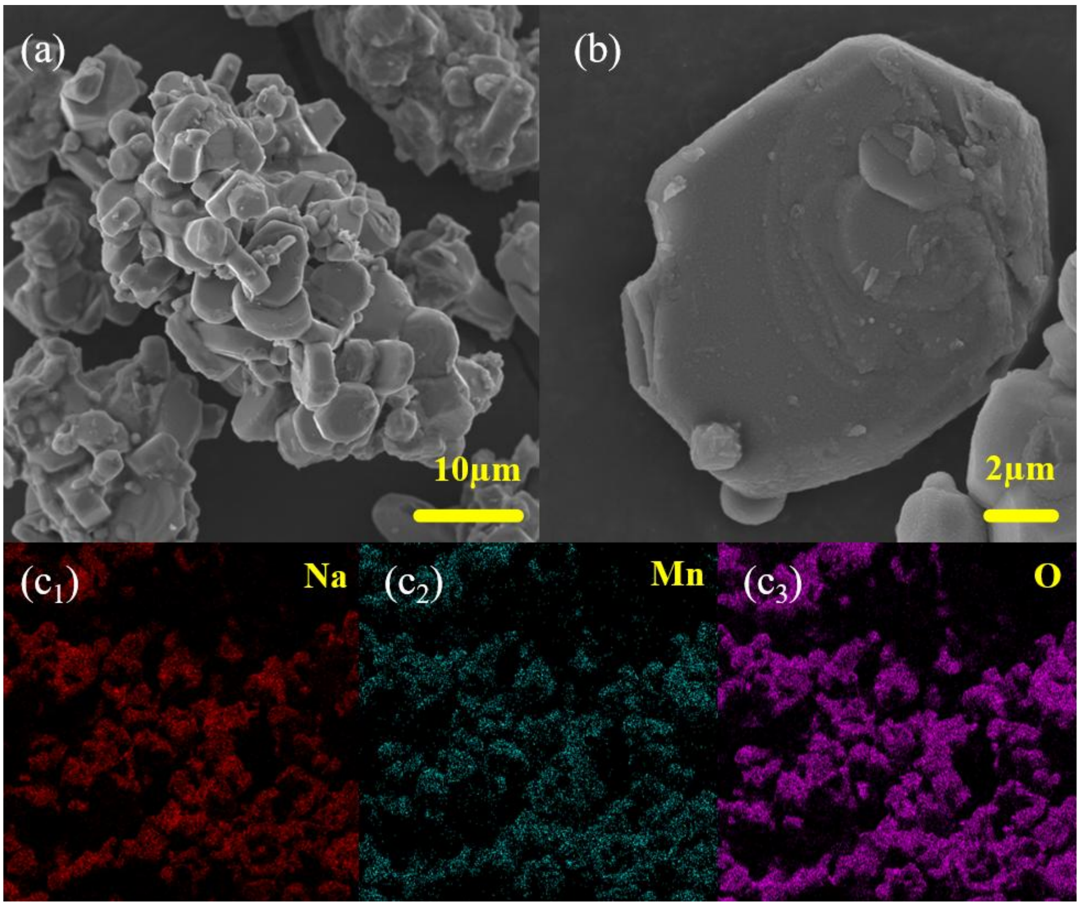

Figure S2. (a-b) SEM images of NLM at different magnifications. (c1-c3) Elemental mapping results.

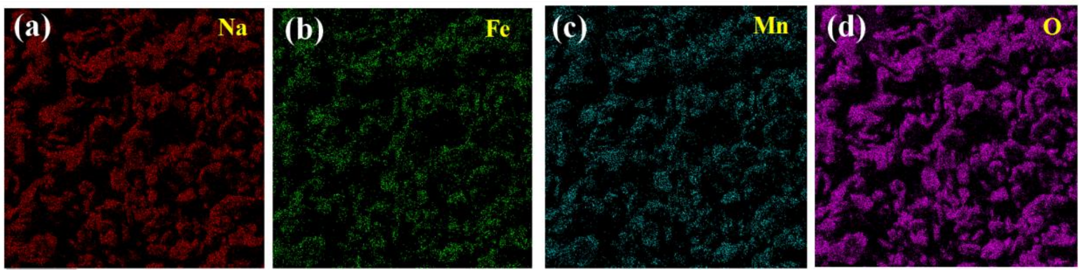

Figure S3. Elemental mapping results of NLFM.

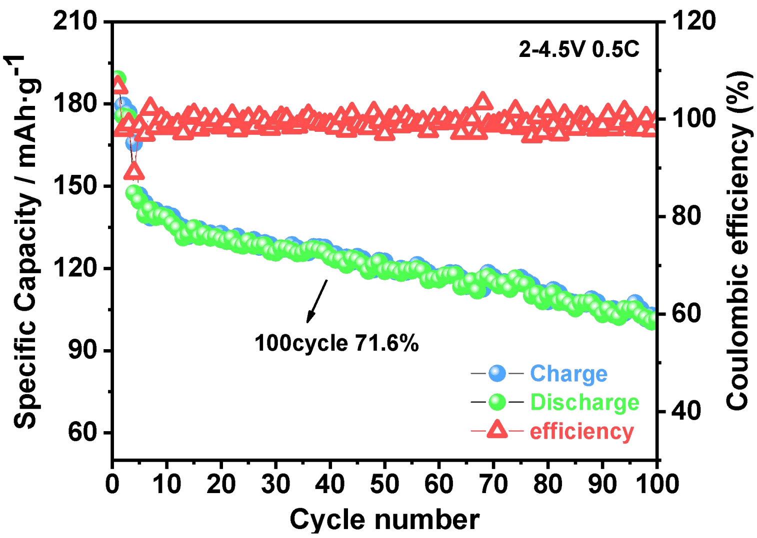

Figure S4. Cycling performance of NLFM at 0.5 C.

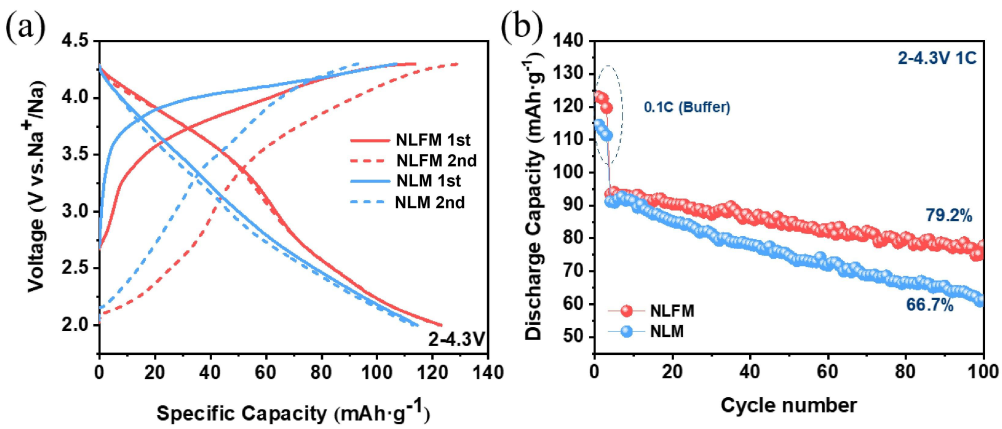

Figure S5. (a) The first two cycles, and (b) Cycling performance of NLM at 0.1 C in a voltage range of 2−4.3 V.

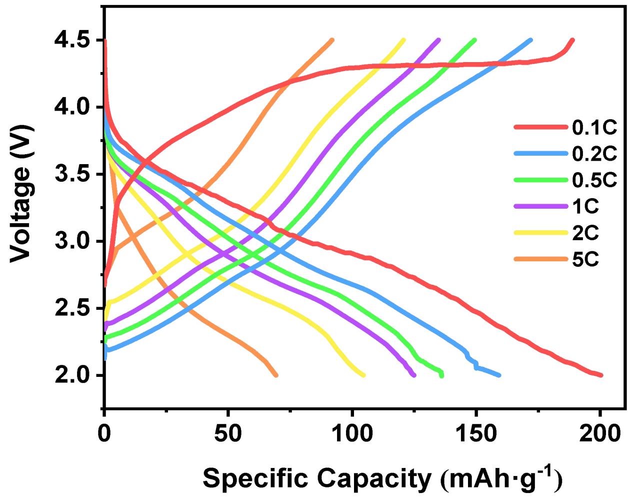

Figure S6. The first-cycle curves of NLFM at 0.1, 0.2, 0.5, 1.0, 2.0, and 5.0 C.

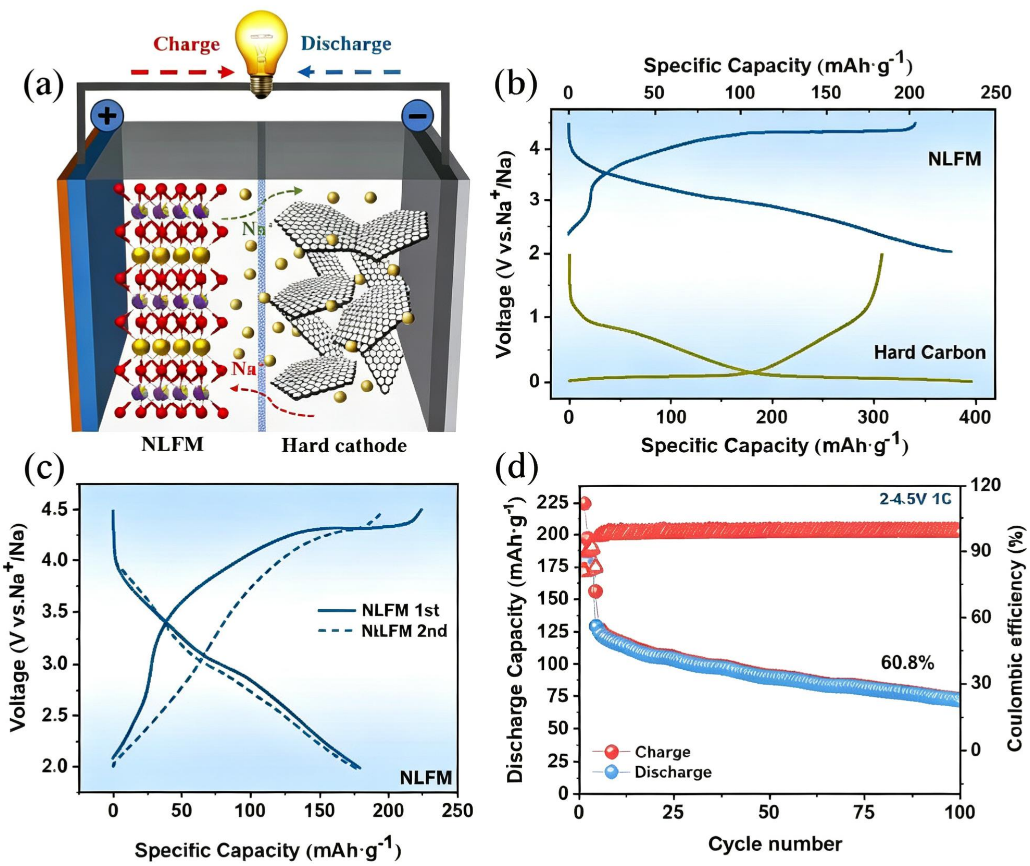

Figure S7. (a) The schematic of full-cell. (b) Galvanostatic charge/discharge curves of hard carbon anode and NLFM. (c) Galvanostatic charge/discharge curves and (d) cycle performance of the pouch full cell at 0.1 and 1C.

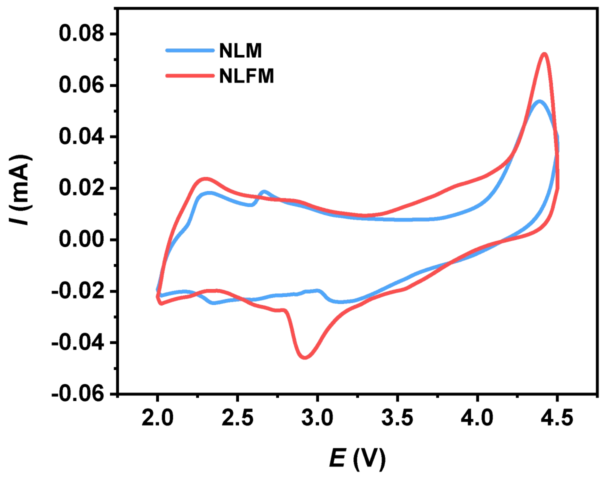

Figure S8. The first-cycle CV curves of NLM and NLFM at 0.1 mV s^{-1}.

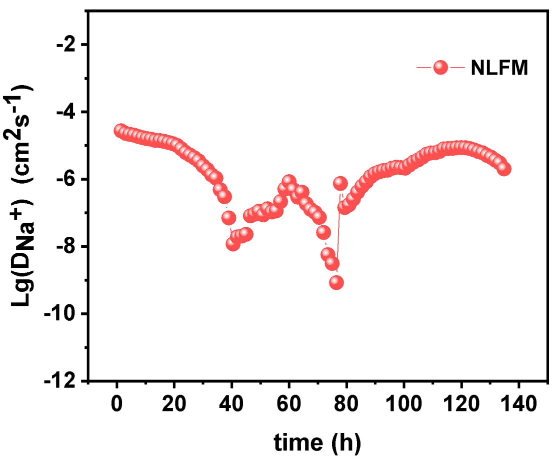

Figure S9. The diffusion coefficients of sodium ion of NLFM.

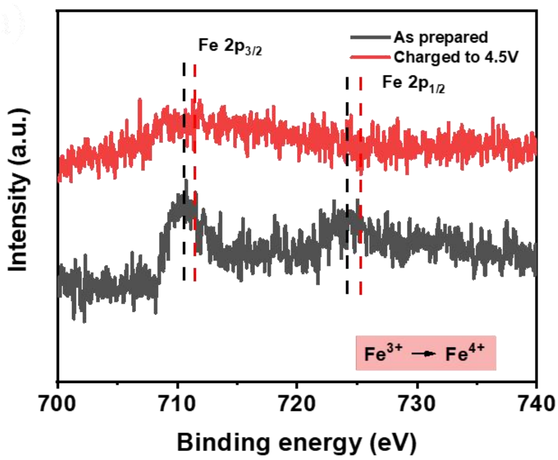

Figure S10. High-resolution Fe 2p of NLFM before and after charging to 4.5 V.

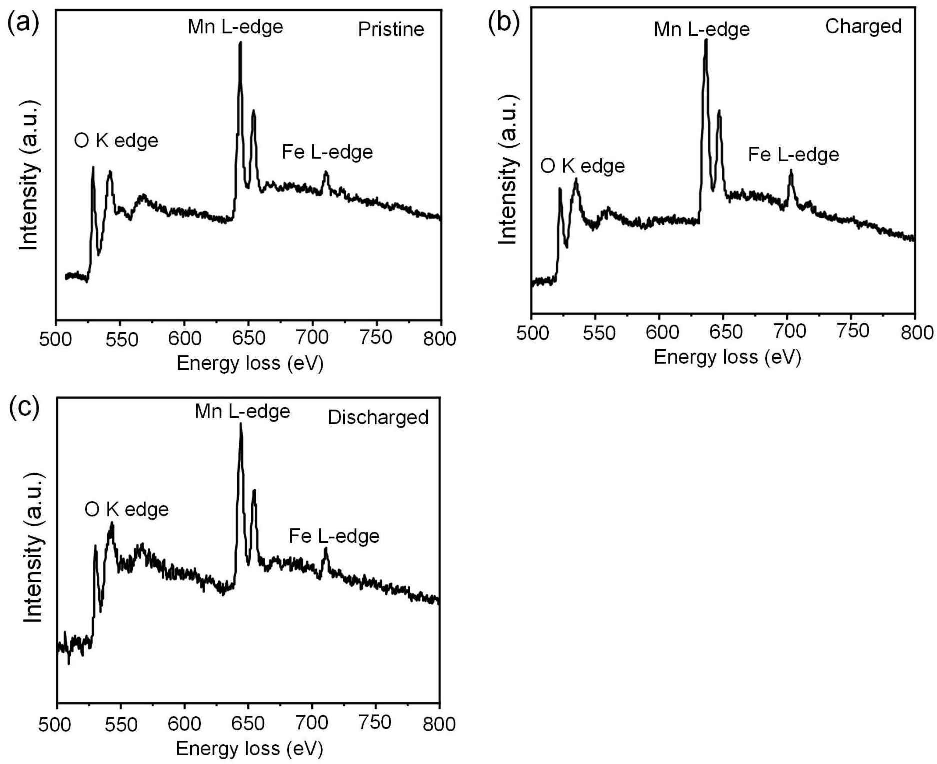

Figure S11. EELS spectra of (a) Pristine NLFM, (b) fully charged to 4.5 V after 50 cycles at 1C, and (c) fully discharged to 2.0 V after 50 cycles at 1C.

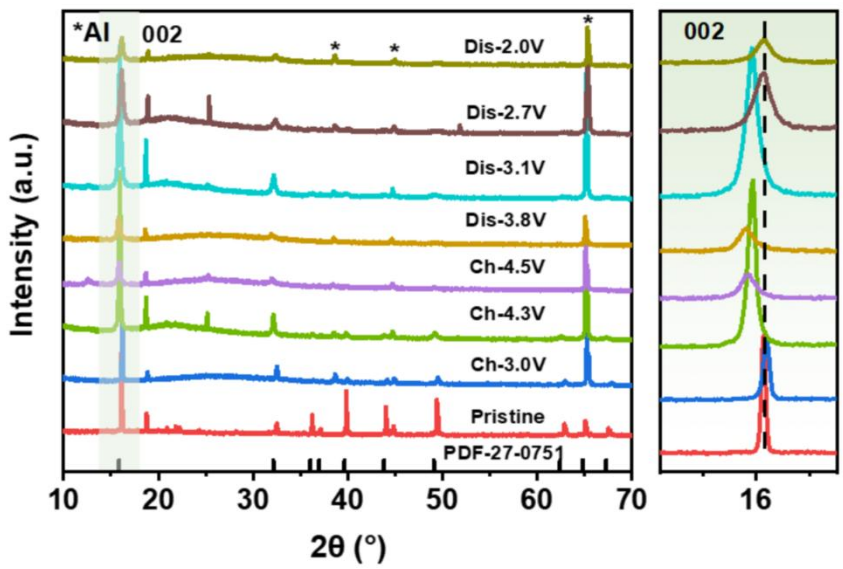

Figure S12. The first charge-discharge cycle of NFM electrode at 0.1 C, different cut-off voltages were selected, and ex-situ XRD patterns were collected.

Table S1. Joint Rietveld refinement results of XRD patterns for the NLFM.

P2 Phase (space group $P6_3/mmc$)					
	Atom	**x**	**y**	**z**	**frac.**
Atomic Occupancies	Na_1	0.0000	0.0000	0.2500	0.266
	Na_2	0.6667	0.3333	0.2500	0.40
	Mn_1	0.0000	0.0000	0.0000	0.666
	Li_1	0.0000	0.0000	0.0000	0.167
	Fe_1	0.0000	0.0000	0.0000	0.167
	O	0.6667	0.3333	0.0714	1.0

Table S2. Lattice parameters of NLM and NLFM.

Lattice Parameters					
Sample	a=b/Å	c/Å	TM-O bond length (Å)	Na-O distance (Å)	Na layer spacing (Å)
NLM	2.8673	11.0333	1.92±0.02	2.45±0.03	3.18±0.02
NLFM	2.8825	11.1361	1.96±0.02	2.51±0.03	3.26±0.02

Table S3. The calculated crystallite size and microstrain of NLM and NLFM.

Sample	Crystallite size D (nm)	Microstrain ε (%)
NLM	78±5	0.21±0.02
NLFM	96±5	0.12±0.02

Table S4. Quantitative Fe/Mn ratio from EDS mapping results.

Element	Weight % (average ± std.)	Atom % (normalized to TM)
Mn	36.2±0.6	80.1±0.5
Fe	9.1±0.3	19.9±0.5
Na	14.5±0.4	_

Table S5. Comparison of electrochemical performance of NLFM with recently reported layered oxide cathodes for sodium-ion batteries.

Cathode Material	Voltage range (V)	Specific capacity ($mAh \cdot g^{-1}$)	Reversible capacity ($mAh \cdot g^{-1}$)	Ref.
P2-$Na_{0.67}Fe_{0.35}Cu_{0.15}Mn_{0.5}O_2$	2-4.0	137.5 (0.1 C)	83.5 (100^{th}, 1 C)	1
P2-$Na_{2/3}Ni_{1/3}Mn_{2/3}O_2$	1.5-4.5	228 (0.05 C)	70.5 (100^{th}, 1 C)	2
P2-$Na_{0.67}Ni_{0.33}Mn_{0.56}Ti_{0.11}O_2$	2-4.3	139.93 (0.1 C)	82.3 (100^{th}, 0.5 C)	3
P2-$Na_{0.6}Mn_{0.97}Fe_{0.03}W_{0.01}O_2$	1.5-4.3	203.02 (0.1 C)	111.2 (100^{th}, 1 C)	4
O3-$Na[Li_{1/3}Mn_{11/18}Ti_{1/18}]O_2$	1.5-4.5	160 (0.2 C)	98.7 (100^{th}, 0.2 C)	5
O3-$NaFe_{0.5}Mn_{0.5}O_2$	2.0-4.2	132 (0.1 C)	61.5 (100^{th}, 0.1 C)	6
P2-$Na_{0.67}Fe_{0.45}Mn_{0.5}Al_{0.03}Sb_{0.02}O_2$	1.5-4.3	143.8 (0.2 C)	73.4 (100^{th}, 0.5 C)	7
P3-$Na_{0.75}Li_{0.08}Cu_{0.25}Mn_{0.66}O_2$	2-4.6	125 (0.1 C)	101 (15^{th}, 0.2 C)	8
P2-$Na_{0.7}1Li_{0.22}Al_{0.05}Mn_{0.73}O_2$	2-4.5	194.4 (0.1 C)	95 (100^{th}, 1 C)	9
O3-$Na[Li_{1/3}Fe_{1/3}Ru_{1/3}]O_2$	1.5-4.1	121 (0.05C)	92.4 (50^{th}, 0.05 C)	10
P2-$Na_{2/3}Li_{1/6}Fe_{1/6}Mn_{2/3}O_2$	**2-4.5**	**220 (0.1 C)**	**90.11 (100^{th}, 1 C)**	**This work**

Table S6. Comparison of Mn 2p spectra for pristine NLM and NLFM.

Sample	Mn^{3+} fraction (%)	Mn^{4+} fraction (%)	Mn^{3+}/Mn^{4+} ratio
NLM	61.3	38.7	1.58
NLFM	31.2	68.8	0.453

References

1. Yan G, Qi Y, Lan C, Hong Y, Fu X, Fang Z. Synthesis and electrochemical performance of Cu-doped P2-type $Na_{0.67}Fe_{0.5-x}Cu_xMn_{0.5}O_2$ cathode materials for sodium-ion batteries. J Energy Storage. 2026; 155: 121557. https://doi.org/10.1016/j.est.2026.121557
2. Risthaus T, Zhou D, Cao X, He X, Qiu B, Wang J, Zhang L, Liu Z, Paillard E, Schumacher G, Winter M, Li J. A high-capacity P2 $Na_{2/3}Ni_{1/3}Mn_{2/3}O_2$ cathode material for sodium ion batteries with oxygen activity. J Power Sources. 2018; 395: 16-24. https://doi.org/10.1016/j.jpowsour.2018.05.026
3. Kang Y, Liu S, Tang H, Xu Y, Zeng Z, Wang M, Hou X, Wang J. Titanium substitution enhancing cycle and rate performances of the P2-type layered transition metal oxide cathodes for sodium-ion batteries. Electrochim Acta. 2026; 562: 148713. https://doi.org/10.1016/j.electacta.2026.148713
4. Hou X, Jin S, Yuan Y, Zhao W, Kang Y, Wang J. Restraining of irreversible phase transition in P2-type layered cathode materials at high potential by W^{6+}-doping. Electrochim Acta. 2025; 536: 146815. https://doi.org/10.1016/j.electacta.2025.146815
5. Qiu Y, Liu Q, Tao J, Yan P, Tan G, Liu F, Wang D, Yu N, Zhang N, Yang Y, Wang W, Wang Y, Cao K, Wang J, Lun Z, Xu C. Enabling the synthesis of O3-type sodium anion-redox cathodes via atmosphere modulation. Nat Commun. 2025; 16: 2343. https://doi.org/10.1038/s41467-025-57665-1
6. Yu L, Ma X, Yang L, Guo Q, Ye S, Ahmad N, Jiang Z, Liang J, Xia J, Peng B, He W, Shi L, Zhang G. Suppressing the high-voltage phase transition in O3-type layered cathode enables ultra-stable sodium-ion batteries. Energy Storage Mater. 2025; 83: 104679. https://doi.org/10.1016/j.ensm.2025.104679
7. Liaqat A, Moeez I, Butt A, Akbar M, Bhatti AHU, Ali G, Chung KY. Stabilizing the structure of P2-$Na_{0.67}Fe_{0.47}Mn_{0.5}Al_{0.03}O_2$ cathodes through Sb-substitution for sodium-ion batteries. J Energy Storage. 2026; 152: 120572. https://doi.org/10.1016/j.est.2026.120572
8. Ronne A, Liu J, Zhang Y, Li M, Lee S, Wang J, Lee GH, Yang W, Yang XQ, Chen-Wiegart YKC, Hu E. Sodium-Ion Battery Cathode with Dominating Copper and Oxygen Redox Chemistry. ACS Energy Lett. 2026; 11: 1827-1834. https://doi.org/10.1021/acsenergylett.5c03483

9. Cai C, Li X, Hu P, Zhu T, Li J, Fan H, Yu R, Zhang T, Lee S, Zhou L, Mai L. Comprehensively Strengthened Metal-Oxygen Bonds for Reversible Anionic Redox Reaction. Adv Funct Mater. 2023; 33: 2215155. https://doi.org/10.1002/adfm.202215155

10. Seol JY, Zhanadilov O, Cho MJ, Kim MG, Voronina N, Myung ST. Coupled Fe^{3+}/Fe^{4+} and oxygen-redox chemistry in O3-Type $Na[Li_{1/3}Fe_{1/3}Ru_{1/3}]O_2$ cathode for sodium-ion batteries. J Power Sources. 2026; 676: 239837. https://doi.org/10.1016/j.jpowsour.2026.239837